Chemical Durability Studies of Perfluorinated Sulfonic Acid Polymers and Model Compounds under Mimic Fuel Cell Conditions

Chun Zhou,[†] Miguel A. Guerra,[‡] Zai-Ming Qiu,[‡] Thomas A. Zawodzinski, Jr.,[§] and David A. Schiraldi*,[†]

Department of Macromolecular Science & Engineering, Department of Chemical Engineering, and the Case Advanced Power Institute, Case Western Reserve University, Cleveland, Ohio 44106, and 3M Fuel Cell Components Program, 3M Corporation, St. Paul, Minnesota 55144

Received July 18, 2007; Revised Manuscript Received September 25, 2007

ABSTRACT: Peroxide radical treatments of a perfluorinated ionomer used in polymer electrolyte membrane (PEM) fuel cells and its small molecule analogues were carried out, along with analysis of the resultant products. Molecules containing terminal carboxylic acids degraded at least 1 order of magnitude faster than noncarboxylate materials; all of the systems did show peroxide-initiated degradation nonetheless. Product analysis suggests that terminal carboxylic acids react according to a sequential chain shortening, consistent with previous studies. Cleavage of side chains from both polymer and model compounds was also observed to be important and in fact may be the dominate pathway in low carboxyl content commercial PEM membranes, based on the following comparison of reactivity and concentration. The relative reactivities of carboxylic chain ends and ether linkages is approximately 500, as calculated using model compounds fluoride generation rates. Commercial perfluorosulfonic acid (PFSA) products contain minimal carboxylic acid end groups, and the side chain concentrations are of 2−3 orders of magnitude higher than carboxylic acid end groups.

1. Introduction

Fuel cells are currently being explored as energy conversion devices which can meet a range of societal needs for transportation, stationary, and portable power. Among the various types of fuel cells under consideration, polymer electrolyte membrane fuel cells (PEMFCs) are a leading technology. PEMFCs make use of proton conducting polymer membranes coated with a composite electrode formed from nanoparticulate electrocatalysts interspersed with ionomer, as is schematically shown in Figure 1.[1,2] The dominant class of polymer electrolyte membranes currently in use are perfluorinated, poly(tetrafluoroethylene)-based polymers bearing perfluoroether side chains which terminate in a sulfonic acid group, or perfluorosulfonic acids (PFSAs).[3] The ionic sulfonic acid groups are believed to self-assemble into channels suitable for proton conduction and water transport necessary for fuel cell operation.[4] Nafion (Nafion is a registered trademark of DuPont for a PFSA ionomer) is currently the benchmark ionomer for PEMFC applications. More in-depth information of the morphology of Nafion is available in a recent review paper.[4]

A critical issue for the commercial success of PEMFCs is their durability, especially for transportation applications. Both academia and the fuel cell industry are actively working to gain understanding of the failure mechanisms of fuel cell systems. Among other fuel cell components, the degradation of membrane is often found to be a significant cause of cell death by the eventual formation of pin-holes and tears, due to the combination of chemical and mechanical degradation.[5,6] Knowledge of membrane chemical degradation mechanisms can provide important material design guidelines to improve the stability

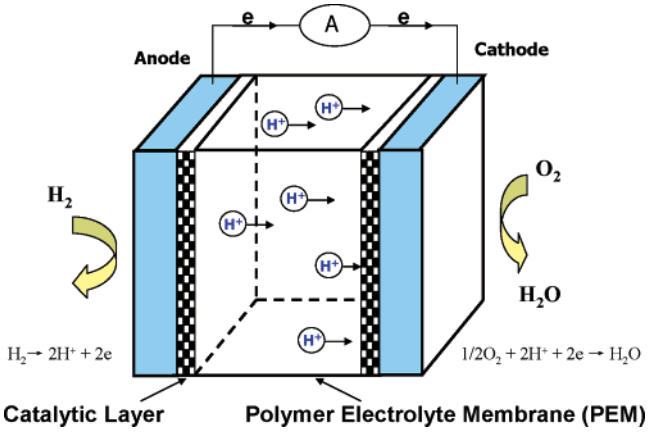

Figure 1. Schematic diagram of a PEM fuel cell.

and the service lifetime of PEMFCs. From the literature it is unclear whether there is a single dominant mode of failure for PEMFC systems. Besides membrane degradation, potential failure modes of other system components include dissolution and aggregation of platinum catalyst particle,[7−10] corrosion of carbon catalyst support,[11,12] and delamination of the electrode and membrane layers.[9] Results of membrane deterioration, such as fluoride evolution in the effluent water, membrane thinning, and pinhole/crack formation are frequently observed in the operating fuel cell systems.[5,13,14] Various mechanical degradation modes have been proposed to explain such observations, including fatigue-type behavior resulting when membranes are subjected to rapid dehydration−rehydration cycles that can be caused by rapid current density changes[13,15] and concentrated stress areas and localized heat spots caused by penetration of catalyst particles into the membrane.[16,17]

The chemical degradation of membranes is thought to play a critical role in the observed fuel cell failures, although the final failure may ultimately result from the interplay between different degradation routes within various fuel cell components.[15] The

* Corresponding author. E-mail: david.schiraldi@case.edu.
[†] Department of Macromolecular Science & Engineering and the Case Advanced Power Institute.
[‡] 3M Corporation.
[§] Department of Chemical Engineering and the Case Advanced Power Institute.

10.1021/ma071603z CCC: $37.00
Published on Web 11/02/2007

Scheme 1. Chain End "Unzipping" Degradation Mechanism

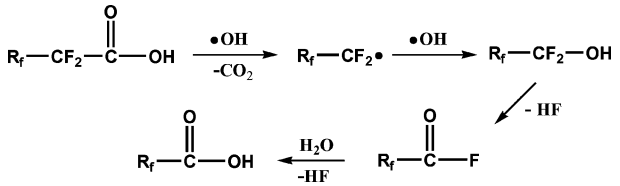

current state of knowledge describing possible chemical mechanisms of degradation for PEM membranes was recently reviewed.[15,18] The majority of authors in the field attribute chemical degradation of PFSA membranes to be caused, at least in part, by exposure to peroxide and hydroxyl radicals known to be produced in these electrochemical devices via incomplete reduction (2 electrons) of O_2. Various membrane chemical structure changes were observed as a result of degradation. Schlick et al.[19] reported the observation of a polymeric radical where the unpaired electron is located on the tertiary backbone carbon atom in Nafion PFSA that is linked to the pendant side chain. Chain end radicals with structures like $R_f-O-CF_2-CF_2^{\bullet}$ were also identified on the side chain radical by electron spin resonance (ESR), when Nafion membranes, saturated with metal counterions, were exposed to UV radiation in the presence of H_2O_2. The reaction between the Fe(III) counterions and sulfonic acid groups on the side chains was proposed to produce such chain end radicals: $R-O-CF_2-CF_2-SO_3^- + Fe(III) \rightarrow R-O-CF_2-CF_2-SO_3^{\bullet} + Fe(II)$, followed by rearrangement via elimination of SO_2 and O_2. Direct soaking of Nafion in 3% (v/v) aqueous H_2O_2 solution for up to 30 days lead to the formation of the S−O−S bond as determined by Fourier transform infrared spectroscopy (FTIR).[20] The S−O−S bond formation was thought to be the result of crosslinking of sulfonic acid groups on the side chains, which subsequently reduces the ductility and proton conductivity. In another study,[21] FTIR studies revealed trace amount of $R-SO_2F$ or S−O−S formation when Nafion was degraded by H_2O_2/Fe(II) solutions; such reagents are commonly known as Fenton's reagent and are widely used to generate hydroxyl and hydroperoxyl radicals.[22] The authors also commented that the side chains were decomposed more easily than the main chain, based on the ^{19}F nuclear magnetic resonance (NMR) integral ratio changes of Nafion repeat units. FTIR, ^{13}C NMR, ^{19}F NMR, and mass spectrometric (MS) analyses of the degradation test solution exhibited fluorinated fragments with the structure largely resembling the derivated Nafion side chain structure.[13,23]

Despite valuable information revealed from the literature cited above, the detailed degradation mechanism(s) leading to the observed chemical structural changes is still poorly understood. One important mechanism was proposed by Curtin et al. to explain the fluoride generation pathway.[24] As shown in Scheme 1, the proposed degradation process starts from the carboxylic acid end groups (−COOH) that may be present in small concentrations in PFSAs. These end groups are unintentionally introduced from the manufacturing process of Nafion and other ionomers via the hydrolysis of the persulfate initiators used in the polymerization of Nafion.[25] The degradation is proposed to proceed by a main chain unzipping mechanism: hydroxyl radicals abstract hydrogen atoms from the terminal −COOH, followed by decarboxylation to form primary perfluorinated radicals. These primary radicals then react with available hydroxyl radicals to form primary fluorinated alcohols, which are highly unstable and rapidly decompose to acyl fluorides with elmination of HF. Subsequent hydrolysis of acyl fluorides yields carboxylic acid ends to re-enter the degradation cycle, shortening the chain by one net carbon unit. Fluorination of end groups

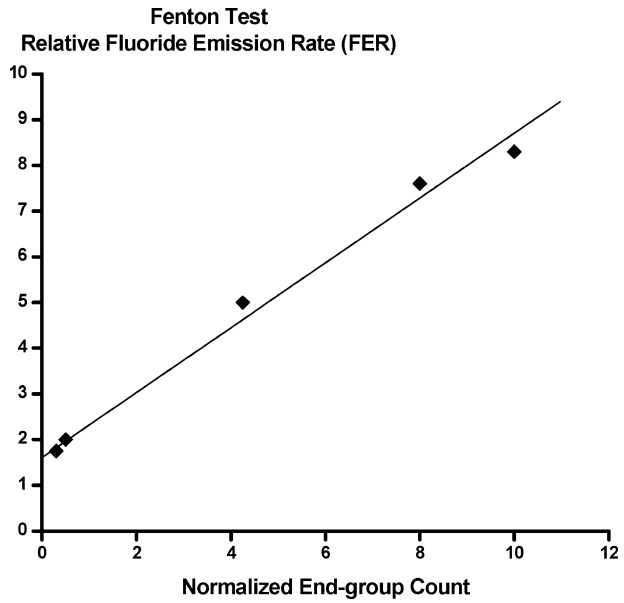

Figure 2. Plot showing relative fluoride emission rate (FER) from Fenton's test as a function of concentration of reactive end-groups (recreated from original plot in ref 25).

leads to the reduction of reactive end group contents, but the fluoride evolution was not eliminated even when the reactive end groups are reduced to be close to zero, as shown in Figure 2.[24,26] A second degradation mechanisms is therefore necessary to account for the significant nonzero fluoride evolution observed when carboxylic acid end groups are eliminated and to potentially explain the structures of PFSA degradation products identified as discussed above.

The present study addresses the need for the construction of a coherent model of PEM polymer degradation mechanisms. In order to gain the benefit of standard chemical methods generally not easily deployed when studying the intractable ionomers, a family of low molecular weight model compounds (MCs) with structural characteristics similar to moieties found in PFSAs was examined. Additionally, the degradation test and products analysis of MCs allow for the comparison of reactivities of different moieties toward degradation. In parallel we report degradation of the benchmark PFSA membrane, Nafion, under the same condition used with the MCs. Relative kinetics of fluoride generation, as well as characterization of degradation products, were considered as mechanistic probes.

2. Experimental Section

Methods and Materials. Nafion 117 membrane (hereafter Nafion) was purchased from Aldrich. Membrane samples were converted to acid form by the following protocol prior to the degradation test: membrane in the form of a film is cleaned by heating in a 1.5% v/v peroxide solution at 70 °C for 1 h, followed by washing the membrane in a hot deionized (DI) water bath (70 °C) for 1 h. The membrane then was boiled in 1 M sulfuric acid for 1 h to convert it to the acid form. The whole process was completed by subsequent washing with 70 °C DI water for 1 h. The structures of model compounds (hereafter MC) considered in this work, along with Nafion ionomers, are given in Figure 3. MC1, perfluoro(2-methyl-3-oxahexanoic) acid, 97%, was purchased from Lancaster Synthesis. MC2, perfluoro(2-methyl-3-oxa-7-sulfonic heptanoic) acid, 96%, MC3, perfluoro(4-sulfonic butanoic) acid, were provided by 3M. MC4, perfluoro-*n*-octanoic acid, 98%, MC5, nonafluorobutanesulfonic acid, and MC6, 1*H*,-perfluorooctane, were purchased from SynQuest Labs. MC7, perfluoro(3-oxahexanoic sulfonic) acid, and MC8, perfluoro(4-methyl-3-oxaoctanoic sulfonic) acid, were provided by 3M. All the MCs were used as received.

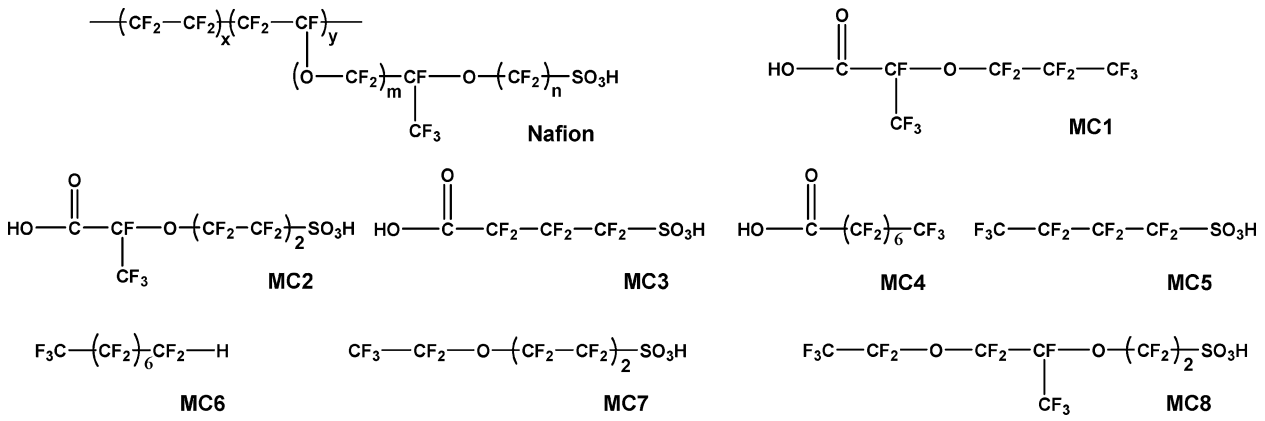

Figure 3. Structures of Nafion (upper left) and various MCs.

Table 1. Concentrations of Reagents Used in Degradation Tests

reagent	concentrations
Fe(II)	1.25 mM (approximately 70 ppm)
H_2O_2	11 mM
MC	100 mM
DI water	50 mL (total)

Ferrous sulfate heptahydrate, 99%, and hydrogen peroxide solution, 30% (w/v), were obtained from Fisher. Total Ionic Strength Adjustment Buffer (TISAB II, with CDTA) solution was purchased from Thermal Orion. Acetonitrile and ammonium acetate, both HPLC grade, were purchased from VWR.

Fluoride Concentration Measurement. Fluoride ion concentration in aqueous solutions was measured using an ion selective electrode (ISE) (Mettler-Toledo, ISE part no. 51340510, meter model number MX300), which was calibrated over the range 0.01−1000 ppm fluoride using NaF aqueous solutions. The detection accuracy limit is at least 0.1 ppm (5.26×10^{-6} M), which still gives a satisfactory calibration curve fit when compared to the theoretical value using the Nernst equation. All of the fluoride concentration data reported here were obtained by a direct measurement method against the calibration curve: The electrode was immersed into a solution containing 2 mL of sample and 2 mL of TISAB II solution (the solution was constantly stirred) and a potential reading of the meter was recorded after equilibrium was reached, typically 5−10 min. The electrode was checked daily by a solution of known fluoride concentration to ensure accuracy and was recalibrated whenever deviation was observed.

Fenton's Degradation Test. The concentrations of MCs and Fenton's reagents are tabulated in Table 1. The exact concentration of H_2O_2 formed in a real fuel cell is very difficult to measure and is a function of many factors such as membrane thickness and location relative to the catalyst layer. A "typical" concentration measured by one group was found to be 10−20 ppm,[27] which translates to approximately 0.5 mM. In this study, 11 mM H_2O_2 concentration was used for accelerated degradation tests.

Degradation Test Procedure of MCs. Each MC was first mixed with a 40 mL aqueous solution containing 1.25 mM ferrous ions by dissolving ferrous sulfate heptahydrate in water (all the concentrations herein are calculated based on the total volume, i.e., the final volume after all the reagents are introduced into the reactor), then the solution was bubbled with nitrogen dry gas for at least 10 min to remove the oxygen that might quench radicals. The solution was subsequently heated to 70 ± 2 °C, and hydrogen peroxide was added through an addition funnel at a slow dropping rate, typically 10−20 drops/min. The reaction mixture was held at approximately 70 °C under nitrogen purge for 24 h, followed by removal of a 2 mL aliquot from the reactor for fluoride concentration measurement. The tests were continued by adding fresh ferrous ions and hydrogen peroxide to react by the same procedure described above, and another fluoride measurement was carried out after an interval of 24 h. The sample process was repeated for 5−6 cycles, for a total of approximately 130 h to complete the test. The data were presented by plotting the amount of fluoride detected as a function of accumulated degradation test time/interval; error bars signify the standard deviation of two to four replicates for various MCs.

Degradation Test Procedure of Nafion. The degradation test started with the acid form of Nafion. The first step was to convert Nafion to its Fe(II)-saturated form by immersing the sample in a 0.1 M $FeSO_4$ solution for 2 h at 70 °C. After the ion exchange, the sample was removed and rinsed with DI water to remove the residual ion exchange solution from the membrane and further blotted dry with paper towels. The samples appeared to be light yellow in color prior to the degradation test. The targeted Fe(II) loadings were quantitative relative to the concentration of sulfonic acids, which was calculated from the equivalent weight of Nafion. The Fe(II)-saturated Nafion samples were added to a round-bottom flask containing DI water, then degassed with dry nitrogen gas for at least 20 min prior to the addition of H_2O_2. The solution was then heated to 70 ± 2 °C, and hydrogen peroxide (concentration 0.1 M based on the total volume of the reaction media) was slowly introduced into the flask to react through an addition funnel. The reaction mixture was held at 70 °C under purge of nitrogen for a certain period of reaction time, typically approximately 35 h. The fluoride concentration measurements were carried out by removal of 2 mL aliquots from the reaction flask. The reaction media was not discarded but used in the following test (2 mL of DI water was added back to the reactor to balance the total volume along with the addition of hydrogen peroxide for the next round of the degradation experiment). The degraded sample (dark brown color) was then converted back to the acid form (colorless) by immersing in 0.5 M H_2SO_4 at 70 °C for 1 h. The next round of the degradation test was then carried out by repeating the procedure described above.

In Situ CO_2 Detection in Degradation Test of MCs. In some degradation tests of carboxylic acid-containing MCs, the purging nitrogen gas was vented to a 50 mM sodium hydroxide solution in a test tube containing phenolphthalein as an indicator (pink when basic, colorless when acidic) to detect the generation of carbon dioxide. Control experiments were run without hydrogen peroxide and without carboxylic acid-containing MCs to demonstrate that no false position CO_2 reading would be obtained.

UV Photolysis Degradation Test. In parallel to the Fenton's reaction, UV photolysis of hydrogen peroxide was exploited as a metal-free source of radical for MC degradation. An advantage of this approach is that it eliminates the iron ions present in Fenton's testing, potentially not present in such high concentrations under actual fuel cell operation. It is well-known in the literature that hydroxyl and peroxyl radicals are generated when hydrogen peroxide is exposed to UV radiation.[19,28] The light source used was an Oriel standard 100 W mercury lamp with a wavelength range of 200−2500 nm. MCs were mixed with DI water (100 mM, total volume of testing samples, 3 mL in a quartz crucible, placed at about 20 cm away from light source) and then further exposed to the UV radiation for 1 h at room temperature, with and without the presence of hydrogen peroxide (400 mM).

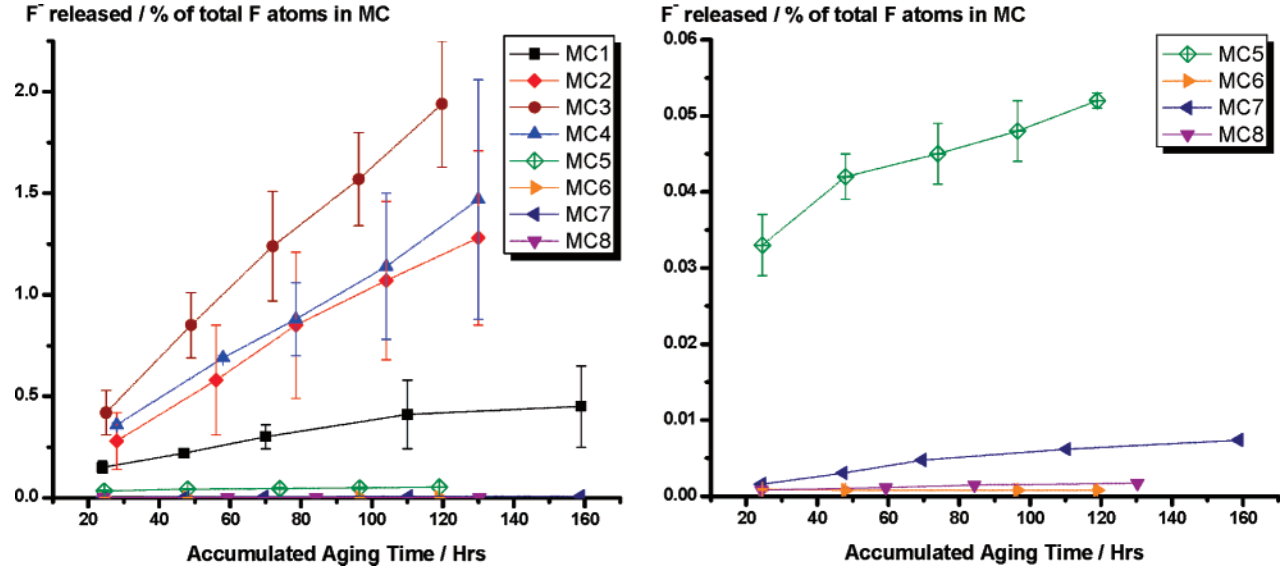

Figure 4. Fluoride evolution from MCs as a function of test time (left, full curve; right, low concentration range).

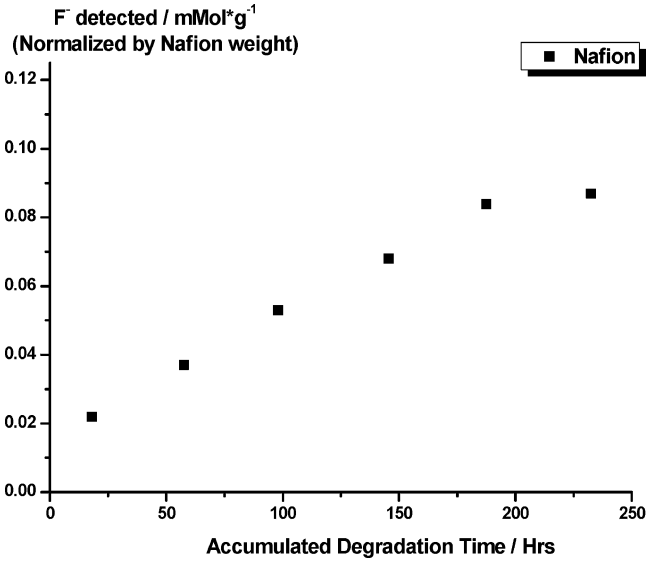

Figure 5. Fluoride evolution from Nafion as a function of test time under Fenton's degradation test.

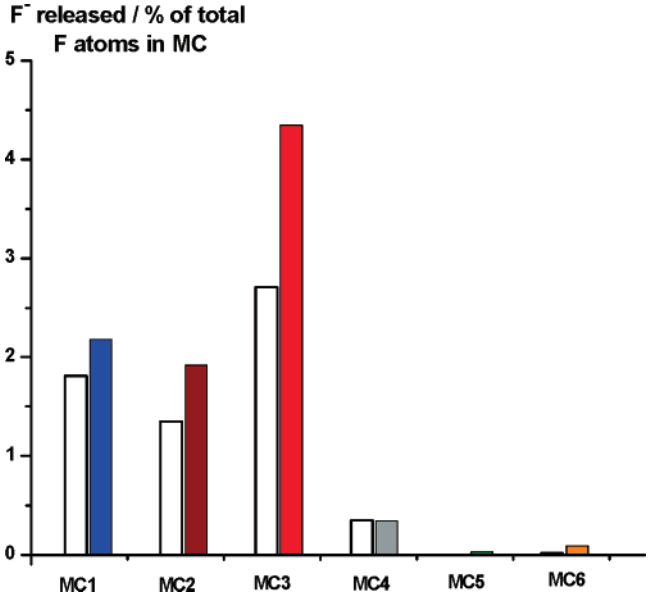

Figure 6. Fluoride evolution from MCs by 1 h UV exposure: unfilled columns represent fluoride generated from UV exposure without H_2O_2 added into the solution; filled columns show the fluoride generated from UV exposure with the presence of H_2O_2.

^{19}F Nuclear Magnetic Resonance (NMR). NMR spectra were obtained using a Varian AS600 600 MHz spectrometer. Acetonitrile-d_3 (Fisher) was used as the solvent for MC treatment experiments; all the chemical shifts are referenced to $CFCl_3$ (defined as 0 ppm) as a standard.

Liquid Chromatography−Mass Spectrometry (LC−MS). The LC−MS analysis was carried out on a Thermo LC−MS system equipped with an HP/Agilent Zorbax column (Eclipse XDB-C18, 2.1 mm × 15 cm). HPLC grade ultrapure water was used to prepare mobile phases. Solvent A: aqueous 6 mM ammonium acetate. Solvent B: 95/5 acetonitrile/water containing 6 mM ammonium acetate. The solvent gradient started with constant 5% B for 5 min, then from 5% B to 100% B in 25 min, followed by holding at 100% B for 5 min. The sample injection volume was 2 μL, and the mobile phase flow rate was 0.25 mL/min. The ionization method is negative ion electrospray. The range of 50−1000 m/z was used for MS scanning.

3. Results and Discussion

3.1. Fluoride Evolution from Fenton's Degradation Tests. Caution has been taken to ensure the accuracy of the fluoride concentration measurement by examining the effect of sample pH, ferrous ion concentration, and ferric ion concentration on measured readings. It was verified that the measurement was not affected by sample pH values when using the TISAB II buffer solution to maintain the desired pH range and good ion background (control experiment data not shown for brevity). When pH > 7, hydroxide ions will interfere with the electrode response to fluoride; for pH < 5, the proton can complex a portion of the fluoride in solution by forming the undissociated acid HF and $(HF_2)^{-1}$ ions. It was also found that the presence of Fe^{2+} between 1 and 50 mM does not interfere with the fluoride measurement when the TISAB II buffer solution is used, while interference from Fe^{3+} at concentrations above 50 mM was observed. This Fe^{3+} interference could be eliminated by a serial sample dilution method, in which an accurate fluoride concentration was obtained by diluting the sample to the point (typically 100-fold dilution) where the concentration of Fe^{3+} was below 25 mM and therefore does not interfere while keeping measuring fluoride concentration well above the detection limit

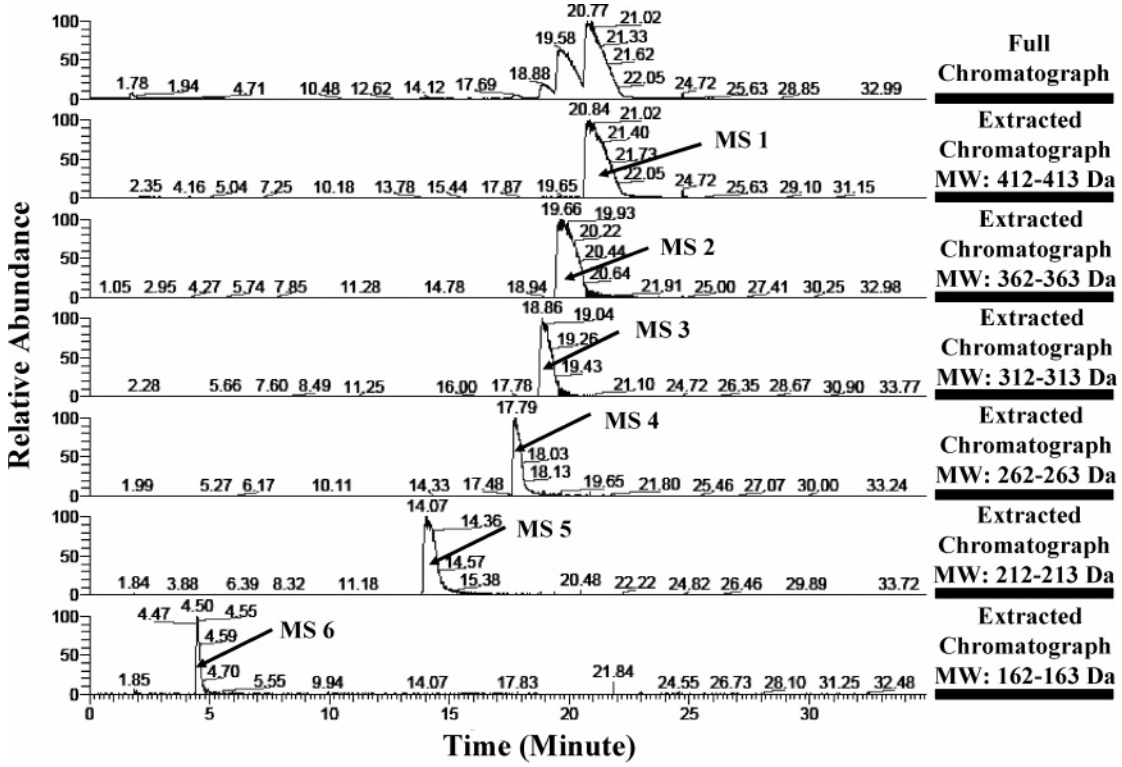

Figure 7. LC chromatographic trace of degraded MC4 reaction product mixture.

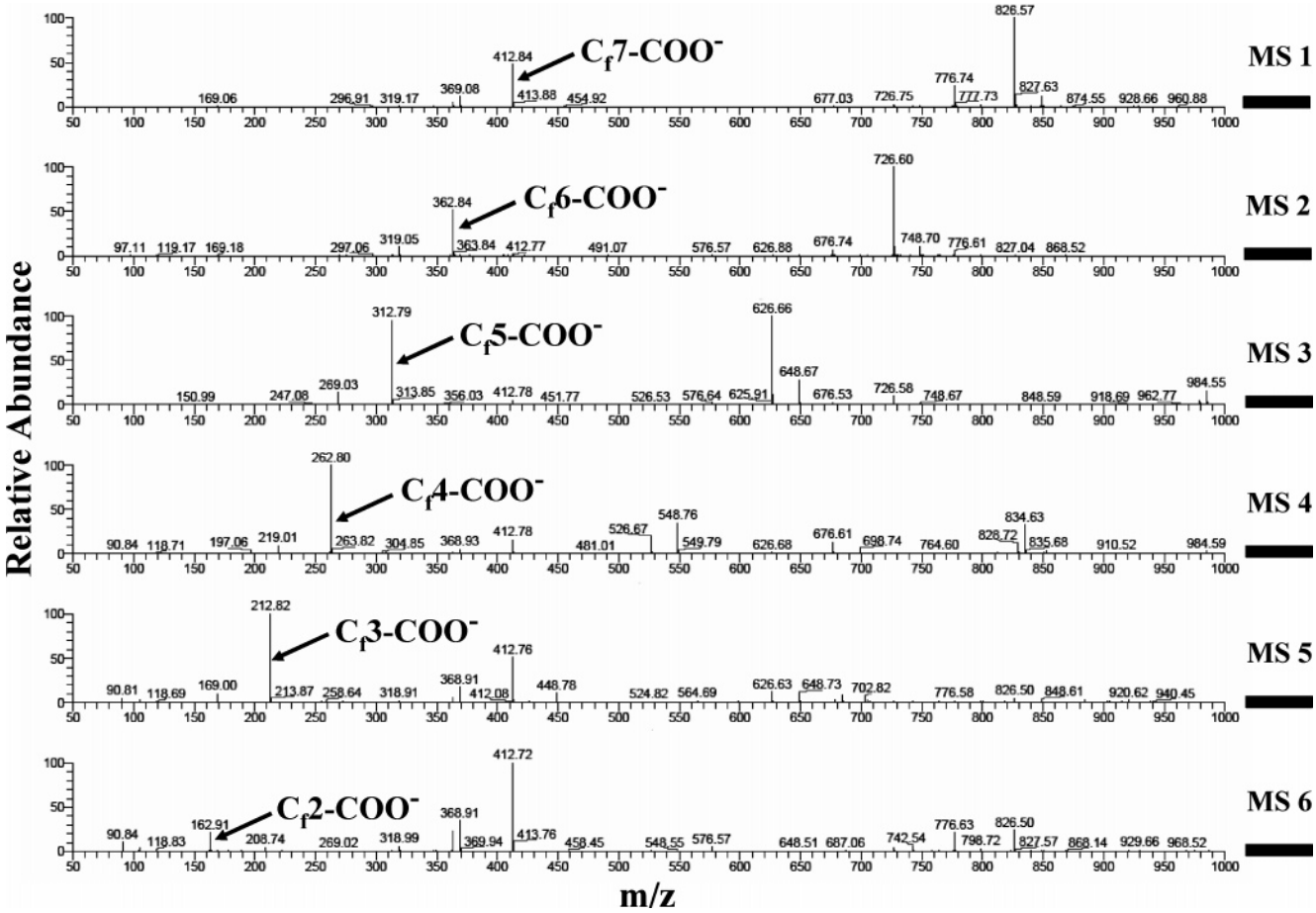

Figure 8. MS spectra of LC trace of a degraded MC4 reaction product mixture at various elution times.

of the electrode. Therefore, if an ISE is used to measure the concentration of fluoride, caution has to be taken to correct for the interference of Fe^{3+} ions.

The fluoride evolution from MCs is plotted in Figure 4. The fluoride concentration is presented as the atomic percentage ratio of fluoride released relative to the total fluorine atoms from

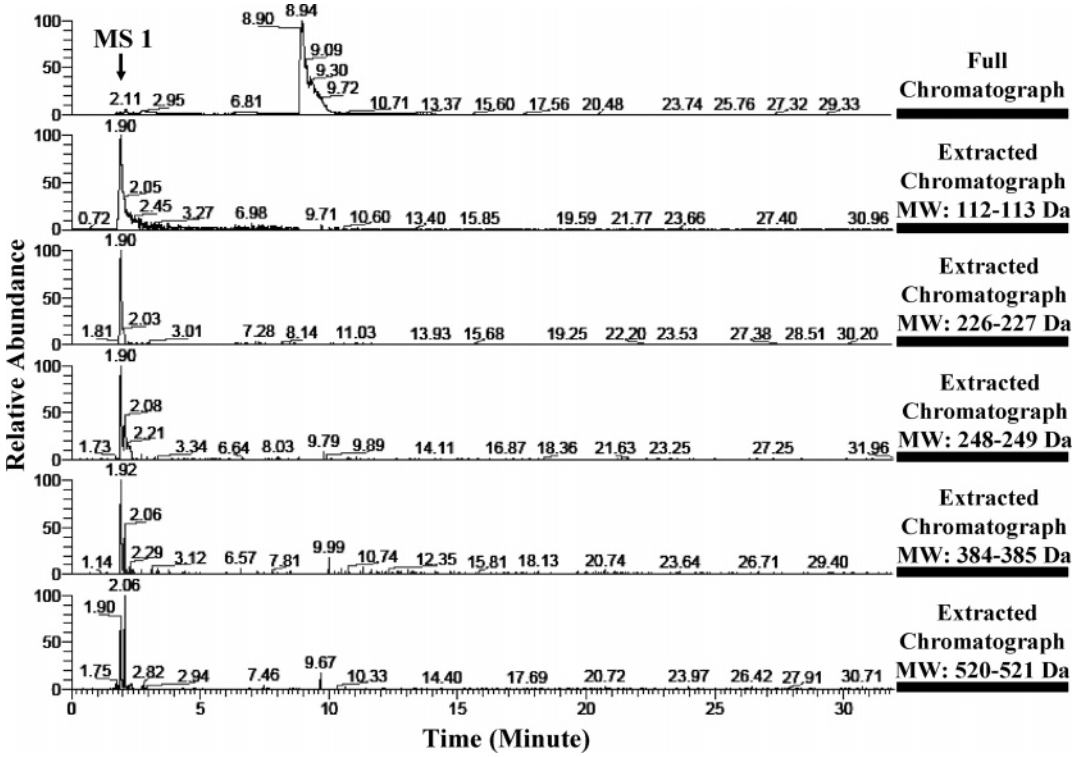

Figure 9. LC chromatographic trace of degraded MC1 reaction product mixture (top). LC traces (relative abundance) of selective ions from TFA (bottom five traces).

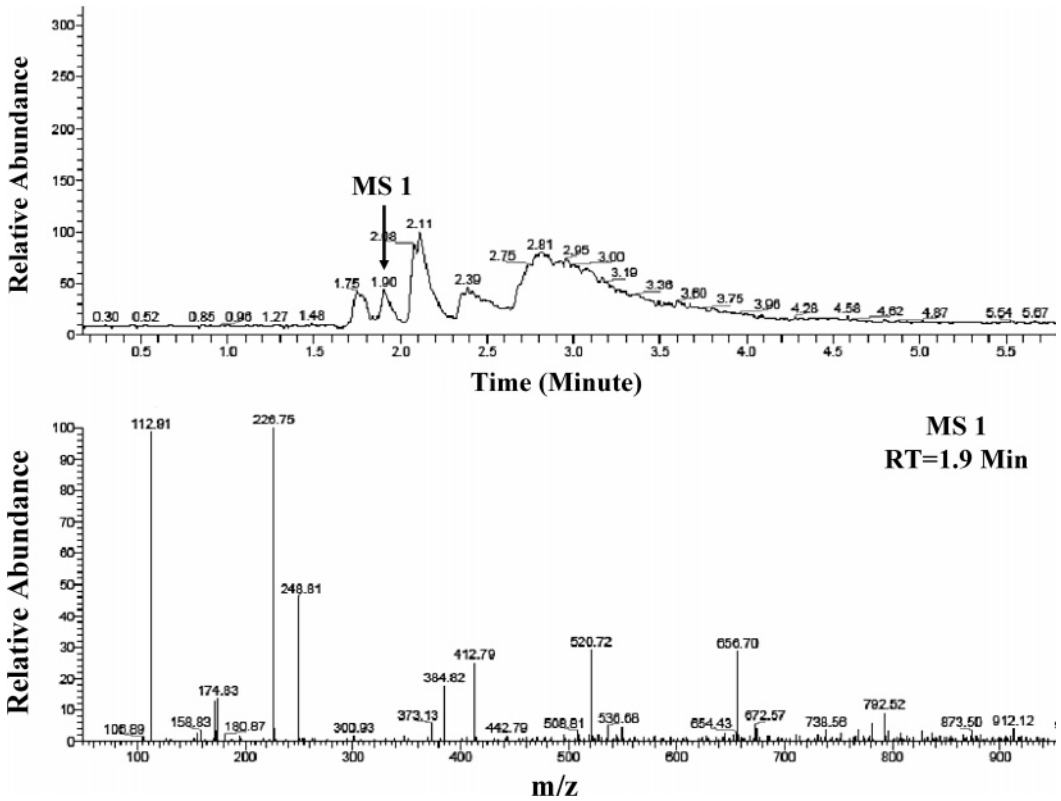

Figure 10. MC1 LC trace (top) and corresponding MS spectrum (bottom) at retention time (RT) = 1.9 min.

each model compound. MCs containing carboxylic acid groups showed significantly higher rates of fluoride generation than those without that functional group. The fluoride evolution of MCs without carboxylic acid groups, MC5 (four-carbon perfluorinated sulfonic acid molecule), MC6 (eight-carbon fluorocarbon molecule containing one hydrogen atom), MC7 (perfluorinated sulfonic acid molecule containing one linear ether linkage), and MC8 (perfluorinated sulfonic acid molecule containing both linear and branched ether linkages), shows the order MC5 > MC7 ∼ MC8 > MC6. The lowest fluoride generation of MC6 is expected due to its low solubility in aqueous solution (phase separation was observed). The relatively higher fluoride release rate observed for MC5 may be due to the fact that MC5 contains fewer fluorine atoms (shorter chain

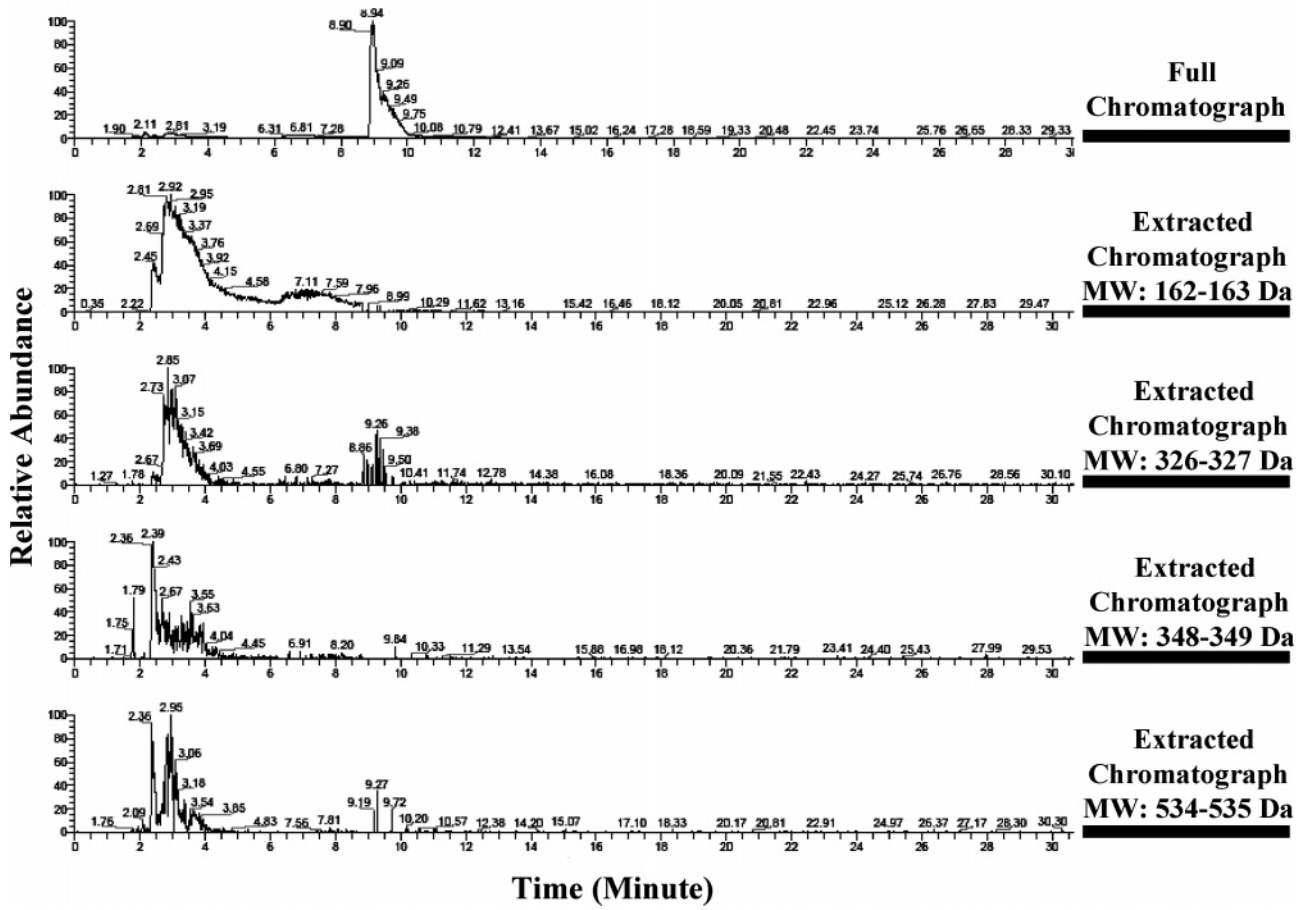

Figure 11. LC chromatographic trace of degraded MC1 reaction product mixture (top). LC traces (relative abundance) of selective ions from PFPA (bottom four traces).

than MC7 and MC8), which may increase the percentage of fluoride release. It is important to note that even for these least reactive model compounds (MC6, MC7, and MC8), nonzero fluoride generation rates were observed. This result implies that fluoride release pathways from PFSAs other than the carboxylic acid end group degradation exist and are kinetically competent (a comparison of MC4 and MC8 degradation rates suggests a factor of 500 difference between carboxylate and noncarboxylate PFSA analogues). This point is highly relevant since MC8 is structurally a close analogue of Nafion, while MC7 is the analogue of other popular commercial PFSAs (nonbranched PTFE and perfluorovinylether sulfonic acid copolymers) manufactured by 3M and Dow. Carboxylic acid-containing MCs, MC1 (branched perfluorinated ether with one terminal carboxylic acid), MC2 (branched perfluorinated ether with both terminal carboxylic acid and sulfonic acid), MC3 (four-carbon fluorocarbon with terminal carboxylic acid and sulfonic acid), and MC4 (eight-carbon fluorocarbon with one terminal carboxylic acid), exhibit the following fluoride generation rate order: MC3 > MC2 ~ MC4 > MC1. The overall trend is monotonic and relatively linear, accounting for as much as 2% of the total fluorine content of the starting materials over 120 h incubation time. The fluoride generation rate of such −COOH containing MCs appeared to be at least 1 order of magnitude higher than MCs without −COOH groups, as shown in Figure 4. Shorter chain MC3 again shows higher fluoride release ratio. Control experiments in the absence of hydrogen peroxide, with or without Fe^{2+} catalyst, failed to generate detectable concentration of fluoride with the MCs.

The fluoride generation from Nafion membrane exposed to Fenton's reagents is shown in Figure 5. The released fluoride is normalized to the sample weight of Nafion sample used, showing a linear trend of fluoride evolution over the testing time. The estimated fluoride evolution rate in current accelerated degradation test is in the order of 1.0×10^{-6} g of fluoride/h cm^{-2}, which is 2 orders of magnitude higher than the fluoride release rate from actual running fuel cells.[5,23] This result shows good validation of the accelerated degradation test method used in this work, i.e., Fe(II) ions are loaded into the membrane and further addition of H_2O_2 can generate attacking radical species inside the membrane. Our control experiment also showed that this degradation method also yielded higher fluoride generation than simply exposing the membrane to a solution containing both Fe(II) ions and H_2O_2 (the "conventional" way of ex situ membrane degradation test), as the degradation might primarily happen on the surface.

3.2. Fluoride Evolution from UV H_2O_2 Photolysis Degradation Test. MC solutions were exposed to UV irradiation to degrade at room temperature, and the fluoride generation was measured. UV irradiation was carried out on MC solutions with and without H_2O_2, and the resultant fluoride generations are shown in Figure 6. For MCs containing carboxylic acid groups (MC1−MC4), UV irradiations led to fluoride generation even without the presence of added H_2O_2, probably due to UV-facilitated decarboxylations that may further trigger structural changes.[29] Higher concentrations of fluorides were generated when H_2O_2 was added to the MC solutions subject to UV irradiation. MC5 and MC6 were found to generate much less fluoride than the −COOH containing MCs, i.e., MC1−MC4, even when UV irradiation was carried with H_2O_2 added. Overall, similar degradation trends were observed between the Fenton's degradation test and UV degradation tests.

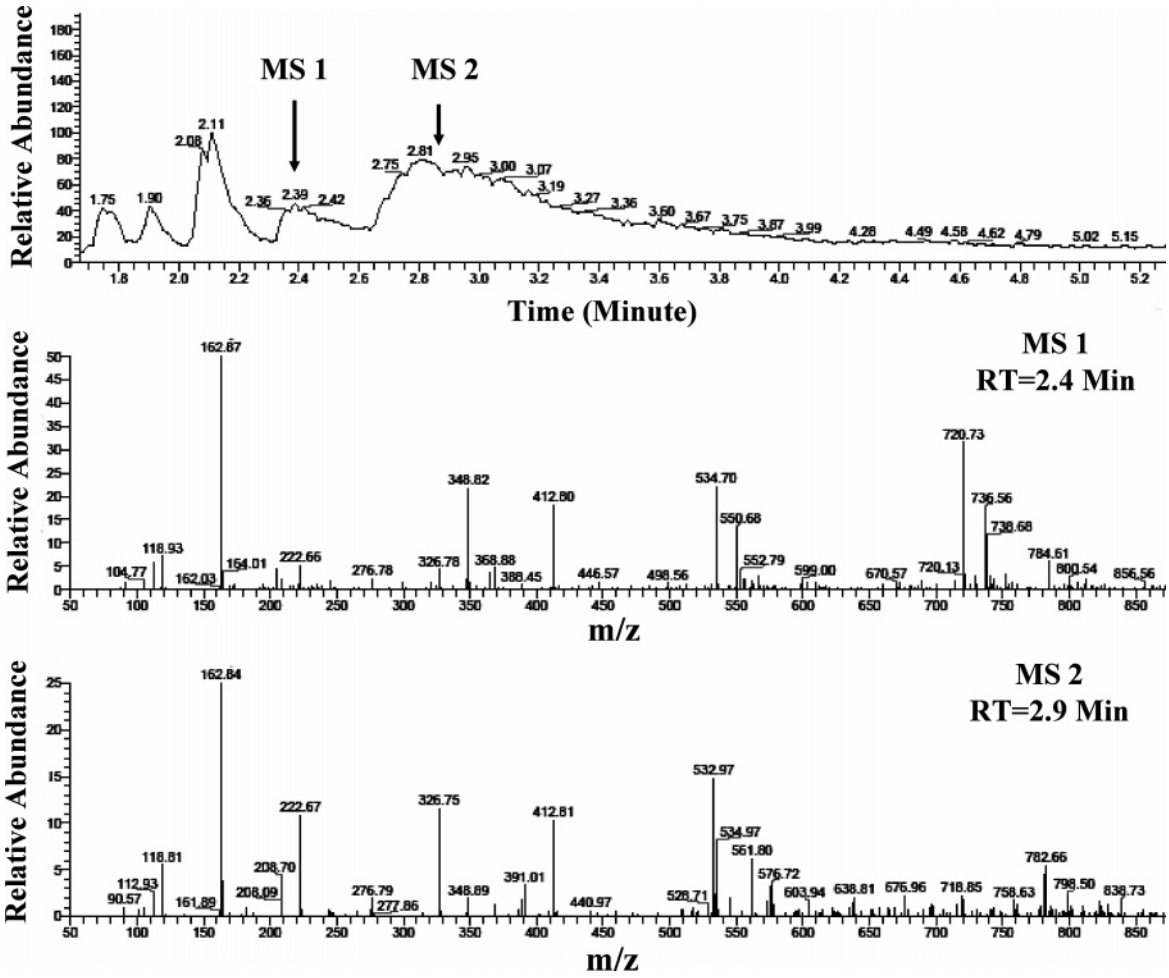

Figure 12. MC1 LC trace (top) and corresponding MS spectra (bottom) at RT = 1.9 and 2.9 min.

Table 2. Tabulated Parent and Adduct Ions of TFA and PFPA

TFA	MW of ions	PFPA	MW of ions
CF_3-COOH	114	CF_3-CF_2-COOH	164
$(TFA - H^+)$	113	$(PFPA - H^+)$	163
$TFA\cdots (TFA - H^+)$	227	$PFPA\cdots (PFPA - H^+)$	327
$(TFA - H^+ + Na^+)\cdots(TFA-H^+)$	249	$(PFPA - H^+ + Na^+)\cdots(PFPA - H^+)$	349
$2(TFA - H^+ + Na^+)\cdots(TFA - H^+)$	385	$2(PFA - H^+ + Na^+)\cdots(PFPA - H^+)$	535
$3(TFA - H^+ + Na^+)\cdots(TFA - H^+)$	521	$3(PFPA - H^+ + Na^+)\cdots(PFPA - H^+)$	721
$4(TFA - H^+ + Na^+)\cdots(TFA - H^+)$	657		

3.3. Degradation Product Analysis of MCs. The chain end unzipping mechanism is widely accepted in the literature. However, the structures of the resultant degradation products have not been confirmed. Chain end unzipping mechanism products were verified by the degradation product analysis of MC4, a molecule that contains only a carboxylic acid group on a linear perfluorinated linear aliphatic chain (R_f-COOH). After the Fenton's test, LC−MS analyses were carried out on the reaction mixture of MC4, shown in Figures 7 and 8.

In Figure 7, the full chromatograph is shown on the top where it is very obvious that there are a series of peaks at different elution times. A specific ion molecular weight can be extracted from the full chromatography trace to show the relative ion intensity of that specific ion at different elution times; the resulting chromatography trace is called an extracted chromatograph hereafter. Such an extraction has been carried out on the full chromatograph of the MC4 reaction mixture. Six ion molecular weight ranges were used to extract the full chromatograph, 412−413, 362−363, 312−313, 262−263, 212−213, and 162−163 Da, and the resulting extracted chromatographs are shown in Figure 7. The full chromatograph is accurately deconvoluted into six peaks at six elution times, and the MS spectrum of each peak at these six elution times were recorded and shown in Figure 8 with the designation of MS 1−MS 6.

MS 1 in Figure 8 exhibits that the peak at this elution time is the intact MC4, where the 413 Da ion is assigned to be the parent ion by losing a proton and forming a negative anion, and the 827 Da ion is assigned to an adduct ion of a molecule of MC4 and a parent ion of MC4. These two ions should serve as good signature ions for solving the MS spectrum with the structure similar to MC4. A close examination of the rest of the MS spectra (MS 2−MS 6) reveals that at those five earlier elution times, the molecular weights of various parent ions differ by 50 Da, and the molecular weights of adduct ions differ by 100 Da, and therefore MS 2 is assigned to be the $C_f6-COOH$ because the difference of this molecule and MC4 ($C_f7-COOH$) is a $-CF_2-$ unit (50 Da). The difference of 100 Da (a net decrease of two $-CF_2-$ units) for the adduct ions and a shorter elution time (a shorter elution time is expected for a molecule with a shorter hydrophobic tail for the reverse phase C18 column used) both confirm this assignment. Similar analogues have also been observed for MS 3−MS 6. The stepwise loss of CF_2 units,

Scheme 2. Proposed Mechanism for MC1 Degradation

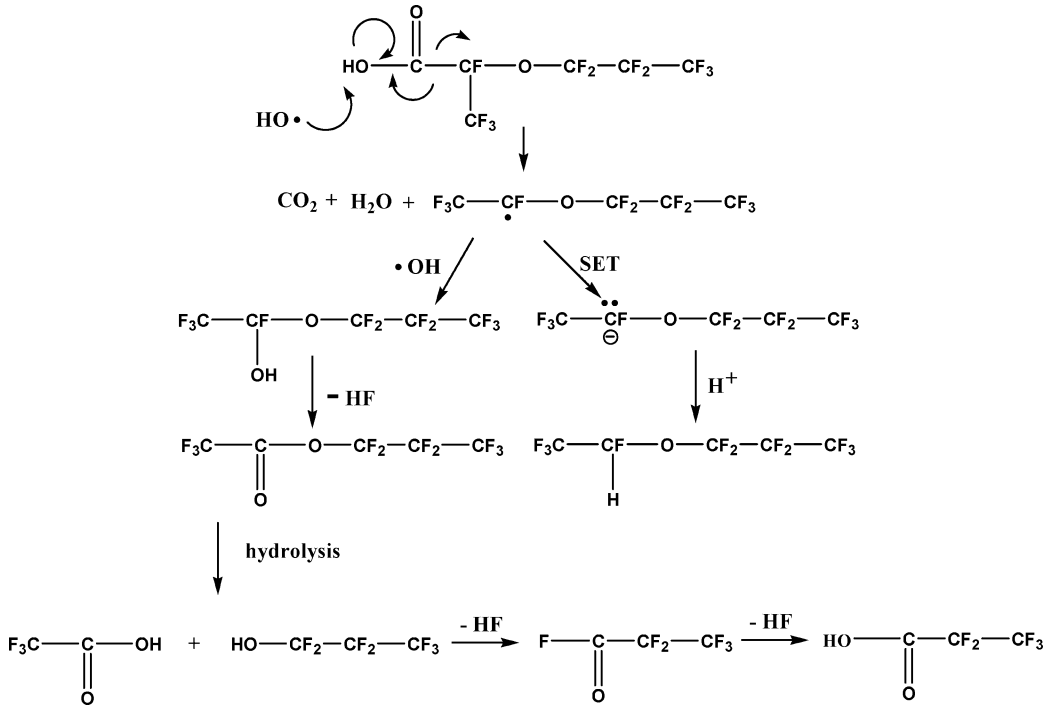

Table 3. Proposed Degradation Products of MC8 with Expect Parent and Adduct Ions

MC8, Product-1 (MC8-PRDT1)

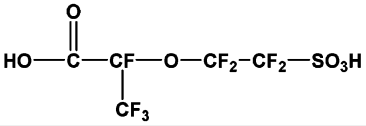

MC8-PRDT1	m/z
(MC8-PRDT1-H^+)	341
(MC8-PRDT1-H^+)-CO_2	297
(MC8-PRDT1-$2H^+$)	170
(MC8-PRDT1-$2H^+$)-CO_2F	277

MC8, Product-2 (MC8-PRDT2)

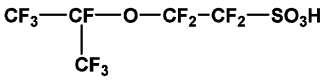

MC8-PRDT2	m/z
(MC8-PRDT2-H^+)	365
MC8-PRDT2 * (MC8-PRDT2-H^+)	731

MC8, Product-3 (MC8-PRDT3)

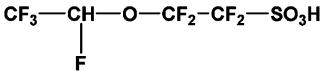

MC8-PRDT3	m/z
(MC8-PRDT3-H^+)	297
MC8-PRDT3 * (MC8-PRDT3-H^+)	595
(MC8-PRDT3-H^++Na^+) * (MC8-PRDT3-H^+)	617

MC8, Product-4 (MC8-PRDT4)

MC8-PRDT4	m/z
(MC8-PRDT4-H^+)	247
(MC8-PRDT4-H^++Na^+) * (MC8-PRDT4-H^+)	517

reforming another terminal carboxylic acid groups, is completely consistent with the unzipping degradation mechanism for degradation of molecules like MC4 under the testing conditions. This LC−MS analysis clearly shows the evolution of the perfluorinated eight carbon acid into its seven through three carbon analogues. Another degradation product, CO_2 gas, was trapped by the method described in the Experimental Section. It was observed that the color of the test tube turned from pink to colorless within 1 h upon the addition of H_2O_2 into the flask. ^{19}F NMR indicated that there were no fluorinated organic compounds in the trapping test tube to cause the observed color change, and the detection of CO_2 again supports the unzipping mechanism.

From fluoride evolution data and the degradation product analysis of MC4, it is clear that terminal carboxylic acid groups are very reactive toward radical attack, and the products of degradation can be readily explained using the chain end unzipping mechanism (Scheme 1). The fate of more complex structures, containing the ether links and branched structures common in PFSAs, also need to be examined. MC1 and MC2 are suitable for such a comparison, since both contain carboxylic acid, ether, and tertiary carbons. In addition, the degradation of MC1 and MC2 will potentially reveal the subsequent degradation fate of the side chains of Nafion, should they be cleaved from the polymer main chain. The LC−MS product analysis results of MC1 are shown in Figures 8−11. LC−MS analysis

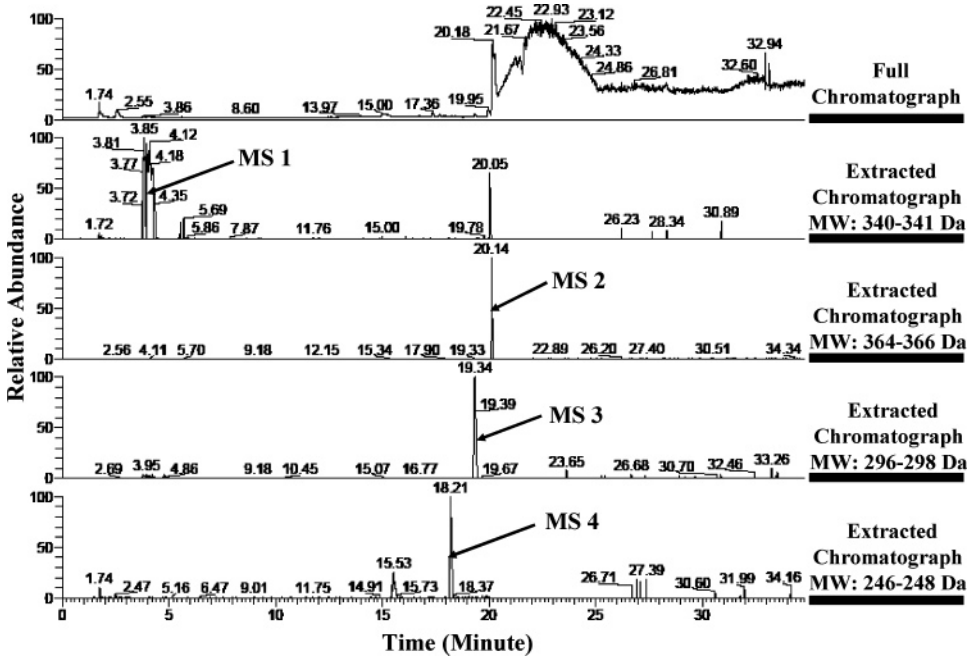

Figure 13. LC chromatographic trace of degraded MC8 reaction product mixture (top). LC traces (relative abundance) of selective ions from proposed products (bottom four traces).

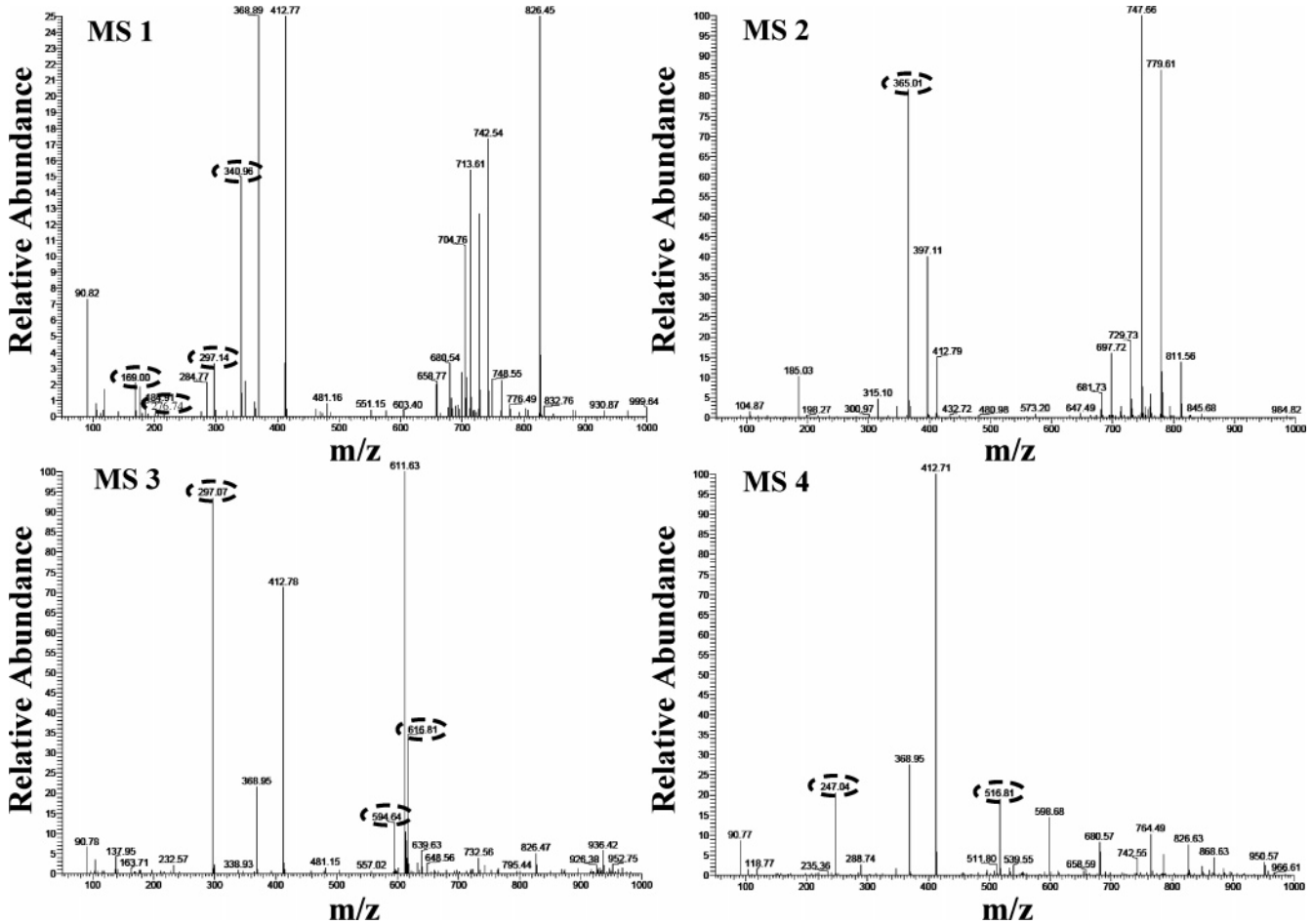

Figure 14. MS spectra marked as MS 1−MS 4 in Figure 11: (top-left) RT = 3.9 min, (top-right) RT = 20.1 min, (bottom-left) RT = 19.3 min, (bottom-right) RT = 18.2 min.

of degraded MC1 identified intact starting material MC1, trifluoroacetic acid (TFA), and pentafluoropropionic acid (PFPA). The parent ions and other corresponding adduct ions for these products are tabulated in Table 2.

From the full LC trace of the MC1 reaction mixture, the large peak at retention time approximately 9.0 min is the intact MC1 reagent. TFA is observed at 1.9 min, and PFPA peak is a broader peak from 2.4 to 4.3 min. It should be mentioned that the other

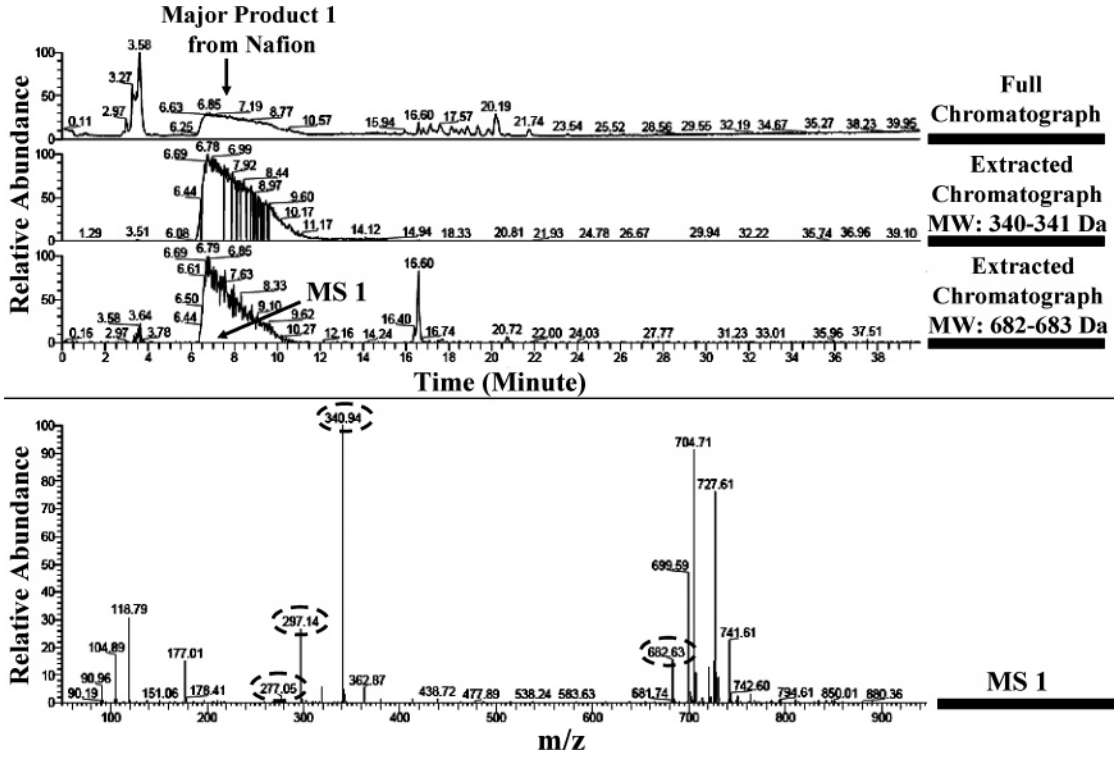

Figure 15. Nafion degradation product LC trace (top three, full and extracted chromatographs) and corresponding MS spectrum (bottom) at RT = 7.7 min.

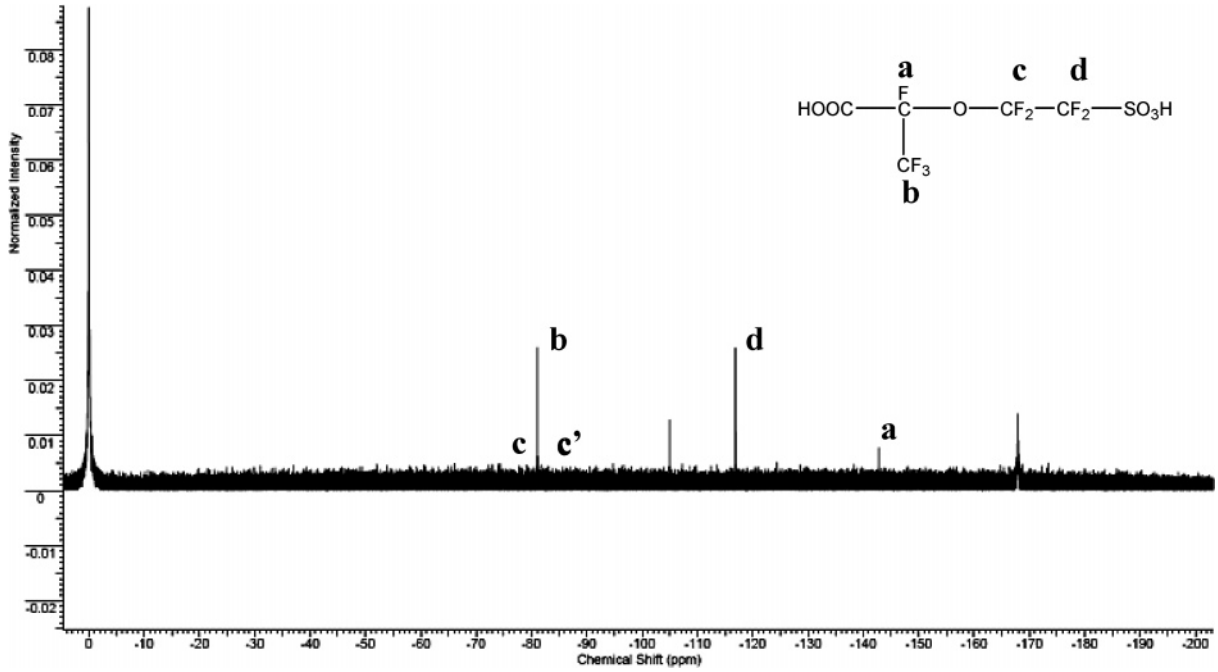

Figure 16. ^{19}F NMR of major product of Nafion degradation from Fenton's degradation test solution.

peaks at 1.7, 2.1, and 6.8 min are identified to be the contaminants present in the LC−MS system background and thus are excluded from the degradation products analysis. Mobile phase empty checks in between data acquisition found similar ion patterns from those peaks, and the expected TFA and PFTA peaks were found from at least three independently degraded samples. The chromatographs extracted by expected ions from TFA are shown in Figure 9, in which the peaks of different ion molecular weights appear at very similar elution times. A similar trend is observed for Figure 11, although the peaks are considerably broader than those of TFA. MS spectra shown in Figures 10 and 12 clearly exhibit the expected ions from TFA and PFTA tabulated in Table 2.

^{19}F NMR analysis of these same reaction products supported the LC−MS assignments (TFA, $-CF_3$ at −76 ppm; PFPA, $-CF_3$ at −82 ppm and $-CF_2-$ at 125 ppm) as well as identifying small concentrations of tetrafluoroethyl, heptafloropropyl ether (−CFH− at about 146 ppm as a doublet of multiplets) as another product. Note that this new ether is not seen in LC−MS, probably due to the fact that in LC−MS the ion acquisition was set to be the negative ion mode. We propose a mechanism which explains the observed reaction products for

Table 4. Proposed Degradation Products of MC7 Based on LC−MS Analysis

Designation, Molecular Weight	Structure
MC7, 416 Da	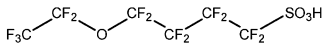
Impurity, 398 Da	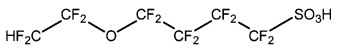
Product A, 276 Da	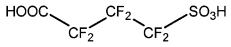
Product B (TFA), 114 Da	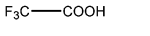
Product C, 392 Da	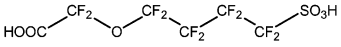
Product D, 300 Da	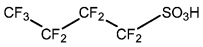

MC1 in Scheme 2. In this mechanism, radical abstraction of a carboxylic acid hydrogen atom initiates decarboxylation of the model compound. The decarboxylated radical intermediate can then undergo single electron transfer (SET) or atom abstraction to produce the observed ether. Capture of a second hydroxyl radical would be expected to produce perfluorinated propyl acetate; we have independently demonstrated that such perfluorinated alkyl acetates will rapidly hydrolyze to the perfluorinated acetic and propionic acids which were identified as MC1 reaction products.

MC8 was chosen as a small molecule analogue to the Nafion polymer itself, substituting a perfluoroethyl group for the polymer backbone. LC−MS analysis of MC8 degradation products identified four significant species in addition to the starting material. LC traces and MS spectra (the expected parent and adduct ions of product 1−4 as tabulated in Table 3 are highlighted with circles) are presented in Figures 13 and 14. The major product appeared to be a fluorinated carboxylic acid compound (MC8, Product-1), which could be expected to result from cleavage of the ether group near the methyl end. Three other structures (Products-2−4) were also identified as being degradation products from MC8 or MC8 degradation product Product-1. One of these reaction products (Product-3) corresponds to a MC1 degradation product as well. What can be clearly stated is that all of the major degradation products of MC8 involves the cleavage of the ether link, analogous to loss of the side chain of Nafion. No evidence for loss of sulfonic acid groups was observed as well.

MC7 was selected as the structural analogue to PFSAs with one ether linkage on the side chain, such as the 3M and Dow products. LC−MS was also carried out to analyze the degradation products. The identified products and impurity compound present are listed in Table 4. Again, the major degradation products of this MC require ether cleavage, similar to the loss of side chains in the polymer itself. It is clear that degradation mechanisms other than the chain end unzipping mechanism are possible in MCs which are structurally analogous to PMSEs. Specifically for MC7 and MC8, structures without carboxylic acid groups also underwent degradation, likely through an ether cleavage reaction.

3.4. Degradation Product Analysis of Nafion. The aqueous extract from Fenton's reagent treatment of Nafion membranes were analyzed using the same LC−MS (Figure 15) and ^{19}F NMR (Figure 16) methods used for the model compounds. The major reaction product from Nafion degradation was identical to Product-1 derived from MC8 (Table 3). Other than the expected ions listed in Table 3, the *m*/*z* value of 682 was assigned to a adduct ion consisting of a deprotonated parent ion and another intact product molecule. The identical degradation product from Nafion running in a fuel cell testing was also independently reported by Healy et al.[23] This result strongly suggests that side chain cleavage in the polymer membrane occurs, just as is the case with its small molecule analogues. It can be argued that the chain end unzipping mechanism in Nafion-like PFSAs might eventually lead to substructures similar to MC1, which can cause the cleavage of side chains following the mechanism described in Scheme 2. This scenario could explain the degradation products observed herein with Nafion. Such a mechanism, however, does not explain the degradation products observed with polymer analogues (MC7 and MC8), nor does it explain the fluoride ion generation rate versus carboxylic acid end group presented in Figure 2. These results would require that a second mechanistic pathway exist for fluoride generation. Fluoride generation can be readily produced during the peroxide degradation of noncarboxylic acid containing small molecule analogues as discussed above, and this degradation pathway primarily proceeds through ether cleavage.

4. Conclusions

With the combination of the product analyses with the relative fluoride generation rates in this study and the published results correlating fluoride generation with carboxyl chain ends in Nafion, a viable model for PFSA radical degradation presents itself: (1**)** To the extent that backbone carboxylic acid groups exist in a PEM membrane, those groups will serve as the preferred sites of attack. (2) Ether linkages, which connect the ionomeric side chains groups to PTFE backbones are also viable points of attack for peroxide radicals and can lead to side chain cleavage. (3) The rate of reaction at carboxylic acid end groups (CEGs) appears to be approximately 500 times that of ether cleavage. Commercial PFSA products contain minimal CEGs, and the side chain concentrations are of 2−3 orders of magnitude higher than CEGs based on the reported molecular weight range of 250K−1 000K.[4] The side chain ether attack can become the dominant mechanism for polymer degradation, consistent with the previously published nonzero fluoride intercept data for a membrane with highly modified fuel cell membrane polymers.

Acknowledgment. This research was supported in part by the Department of Energy, Cooperative Agreement No. DE-FC36-03GO13098. DOE support does not constitute an endorsement by DOE of the views expressed in this paper. Thoughtful discussions with Mike Hicks, Mike Yandrasits, and Tom Kestner of 3M Company are gratefully appreciated.

References and Notes

(1) Rikukawa, M.; Sanui, K. Proton-conducting polymer electrolyte membranes based on hydrocarbon polymers. *Prog. Polym. Sci.* **2000**, *25* (10), 1463−1502.
(2) Gottesfeld, S.; Zawodzinski, T. A. Polymer electrolyte fuel cells. *Adv. Electrochem. Sci. Eng.* **1997**, *5*, 195−301.
(3) Souzy, R.; Ameduri, B. Functional fluoropolymers for fuel cell membranes. *Prog. Polym. Sci.* **2005**, *30* (6), 644−687.
(4) Mauritz, K. A.; Moore, R. B. State of understanding of Nafion. *Chem. Rev.* **2004**, *104* (10), 4535−4585.
(5) Liu, W.; Ruth, K.; Rusch, G. Membrane Durability in PEM Fuel Cells. *J. New Mater. Electrochem. Syst.* **2001**, *4* (4), 227−232.
(6) Liu, W.; Crum, M. Effective testing matrix for studying membrane durability in PEM fuel cells: part I. Chemical durability. *ECS Trans.* **2006**, *3*, (1, Proton Exchange Membrane Fuel Cells 6), 531−540.

(7) Bi, W.; Gray, G. E.; Fuller, T. F. PEM Fuel Cell Pt/C Dissolution and Deposition in Nafion Electrolyte. *Electrochem. Solid-State Lett.* **2007**, *10* (5), B101−B104.
(8) Darling, R. M.; Meyers, J. P. Kinetic model of platinum dissolution in PEMFCs. *J. Electrochem. Soc.* **2003**, *150* (11), A1523−A1527.
(9) Bosnjakovic, A.; Schlick, S. Spin Trapping by 5,5-Dimethylpyrroline-*N*-oxide in Fenton Media in the Presence of Nafion Perfluorinated Membranes: Limitations and Potential. *J. Phys. Chem. B* **2006**, *110* (22), 10720−10728.
(10) Luo, Z.; Li, D.; Tang, H.; Pan, M.; Ruan, R. Degradation behavior of membrane-electrode-assembly materials in 10-cell PEMFC stack. *Int. J. Hydrogen Energy* **2006**, *31* (13), 1831−1837.
(11) Stevens, D. A.; Hicks, M. T.; Haugen, G. M.; Dahn, J. R. Ex Situ and In Situ Stability Studies of PEMFC Catalysts. *J. Electrochem. Soc.* **2005**, *152* (12), A2309−A2315.
(12) Cai, M.; Ruthkosky, M. S.; Merzougui, B.; Swathirajan, S.; Balogh, M. P.; Oh, S. H. Investigation of thermal and electrochemical degradation of fuel cell catalysts. *J. Power Sources* **2006**, *160* (2), 977−986.
(13) Tang, H.; Peikang, S.; Jiang, S. P.; Wang, F.; Pan, M. A degradation study of Nafion proton exchange membrane of PEM fuel cells. *J. Power Sources* **2007**, *170* (1), 85−92.
(14) Aoki, M.; Uchida, H.; Watanabe, M. Decomposition mechanism of perfluorosulfonic acid electrolyte in polymer electrolyte fuel cells. *Electrochem. Commun.* **2006**, *8* (9), 1509−1513.
(15) Collier, A.; Wang, H.; Yuan, X. Z.; Zhang, J.; Wilkinson, D. P. Degradation of polymer electrolyte membranes. *Int. J. Hydrogen Energy* **2006**, *31* (13), 1838−1854.
(16) Huang, C.; Tan, K. S.; Lin, J.; Tan, K. L. XRD and XPS analysis of the degradation of the polymer electrolyte in H_2-O_2 fuel cell. *Chem. Phys. Lett.* **2003**, *371* (1,2), 80−85.
(17) Taniguchi, A.; Akita, T.; Yasuda, K.; Miyazaki, Y. Analysis of electrocatalyst degradation in PEMFC caused by cell reversal during fuel starvation. *J. Power Sources* **2004**, *130* (1−2), 42−49.
(18) Schiraldi, D. A. Perfluorinated polymer electrolyte membrane durability. *Polym. Rev.* **2006**, *46* (3), 315−327.
(19) Kadirov, M. K.; Bosnjakovic, A.; Schlick, S. Membrane-Derived Fluorinated Radicals Detected by Electron Spin Resonance in UV-Irradiated Nafion and Dow Ionomers: Effect of Counterions and H_2O_2. *J. Phys. Chem. B* **2005**, *109* (16), 7664−7670.
(20) Qiao, J. L.; Saito, M.; Hayamizu, K.; Okada, T. Degradation of perfluorinated ionomer membranes for PEM fuel cells during processing with H_2O_2. *J. Electrochem. Soc.* **2006**, *153* (6), A967−A974.
(21) Kinumoto, T.; Inaba, M.; Nakayama, Y.; Ogata, K.; Umebayashi, R.; Tasaka, A.; Iriyama, Y.; Abe, T.; Ogumi, Z. Durability of perfluorinated ionomer membrane against hydrogen peroxide. *J. Power Sources* **2006**, *158* (2), 1222−1228.
(22) Walling, C. Fenton's reagent revisited. *Acc. Chem. Res.* **1975**, *8* (4), 125−31.
(23) Healy, J.; Hayden, C.; Xie, T.; Olson, K.; Waldo, R.; Brundage, M.; Gasteiger, H.; Abbott, J. Aspects of the chemical degradation of PFSA ionomers used in PEM fuel cells. *Fuel Cells (Weinheim, Ger.)* **2005**, *5* (2), 302−308.
(24) Curtin, D. E.; Lousenberg, R. D.; Henry, T. J.; Tangeman, P. C.; Tisack, M. E. Advanced materials for improved PEMFC performance and life. *J. Power Sources* **2004**, *131* (1−2), 41−48.
(25) Bro, M. I.; Sperati, C. A. End groups in tetrafluorethylene polymers. *J. Polym. Sci.* **1959**, *38*, 289−95.
(26) Escobedo, G. Strategies to improve the durability of perfluorosulfonic acid membranes for PEM fuel cells. *KFTCA International Symposium*, Washington, DC, December 8−9, 2005.
(27) Liu, W.; Zuckerbrod, D. In situ detection of hydrogen peroxide in PEM fuel cells. *J. Electrochem. Soc.* **2005**, *152* (6), A1165−A1170.
(28) Hubner, G.; Roduner, E. EPR investigation of HO. radical initiated degradation reactions of sulfonated aromatics as model compounds for fuel cell proton conducting membranes. *J. Mater. Chem.* **1999**, *9* (2), 409−418.
(29) Chen, J.; Zhang, P.-y.; Liu, J. Photodegradation of perfluorooctanoic acid by 185 nm vacuum ultraviolet light. *J. Environ. Sci. (Beijing)* **2007**, *19* (4), 387−390.

MA071603Z